Response of Atmospheric Surface Layer Turbulence to a Partial Solar Eclipse

R. A. ANTONIA, A. J. CHAMBERS, D. PHONG-ANANT, S. RAJAGOPALAN, AND K. R. SREENIVASAN

Department of Mechanical Engineering, University of Newcastle, New South Wales 2308, Australia

Measurements of velocity and temperature fluctuations were made over a period including a solar eclipse of 80% totality to determine the response of surface layer to the change in ground heat flux. The response of the rms velocity fluctuation lags behind that of the rms temperature fluctuation by about 20 min. Although the velocity spectrum exhibits a good inertial subrange for the whole period of observation, the inertial subrange in the temperature spectrum disappears shortly after the start of the eclipse. It is found that during the eclipse the surface layer turbulence approximately follows a continuum of equilibrium states in response to stability changes brought about by the change in surface heat flux.

INTRODUCTION

Since solar radiation is the eventual source of energy input to the atmosphere, the effect of the sudden removal of the incoming radiation is of considerable interest. Since the ground adjusts to a sudden change in radiative heating or cooling from the sun faster than the air above it, the surface layer is first to feel this change. In the case of surface cooling an internal thermal layer [*Townsend*, 1976, p. 379] propagates away from the ground through the surface layer. *Townsend* [1976] describes a tendency to deceleration of the mean flow with, as a most dramatic consequence, the collapse of both the turbulent motion and the mean flow when the Richardson number exceeds a critical value. *Townsend's* [1957] analysis showed that this critical value is of the order of 0.1. In the laboratory, *Nicholl* [1970] has observed such a collapse and reported that although the rate of working of turbulence against gravity was an order of magnitude less than the rate of supply of turbulent energy from the mean shear, it was sufficient to suppress the turbulence in a very short time. In the atmosphere a sudden decrease in the gustiness of the surface wind is observed at sunset with clear skies. Townsend suggests that the depth of the affected region is of the order of the Monin-Obukhov length (about 10 m). A better approximation to a sudden change in surface cooling occurs during a total solar eclipse. On October 23, 1976, some parts of southern and southeastern Australia experienced a total solar eclipse (for a general description, see, for example, *Trainor* [1976]). During this period we were participating in the International Turbulence Comparison Experiment organized by the Council for Scientific and Industrial Research (CSIRO) Division of Atmospheric Physics (Aspendale, Victoria) and conducted at a site near Conargo, 40 km northeast of Deniliquin, in the Riverina district of New South Wales. Although the eclipse at Deniliquin reached only 80% totality and the period following the eclipse merged gradually into the normal sunset period, it still seemed worthwhile to examine the response of both temperature and velocity fluctuations in the surface layer to the decrease in surface heat flux. Ideally, the return to normal sunny conditions following the eclipse would have provided a situation opposite to the one considered here. However, the redeeming features of the present experiment were the fine weather prior to the eclipse and a generally cloudless sky, especially during the eclipse.

Paper number 8C1207.
0148-0227/79/008C-1207$01.00

EXPERIMENTAL CONDITIONS AND INSTRUMENTATION

A detailed description of the site will be given elsewhere. It is sufficient to point out here that the site had a long obstruction-free fetch of about 2 km in the direction of the wind. Mean velocity and temperature were measured at heights of 1, 2, 4, 8, and 16 m above the ground. (These data were supplied to us by the CSIRO.) Both temperature (θ) and horizontal streamwise velocity (u) fluctuations were obtained with the use of cold and hot wires, respectively. Two pairs of hot-cold wire combinations were mounted on a mast at heights of 2 and 4 m. For each pair the separation between the hot and cold wires was about 1 cm. The cold wire was a 0.6-μm Pt-Rh Wollaston wire of approximately 560-Ω resistance. It was operated with a dc-coupled constant current bridge at a current of 0.1 mA. This low value of heating current ensures that the wire is sensitive to temperature fluctuations only. The hot wire was a 5-μm Pt-Rh Wollaston wire operated with a DISA 55M01 anemometer at an overheat ratio of 1.8. Both hot and cold wires were precalibrated in the laboratory and checked for consistency with the wind conditions that prevailed during the experiment. Signals from both wires were passed through DISA 55D26 signal conditioners (to provide the required gain, filtering, and dc offset) before recording them on a 3960A Hewlett-Packard tape recorder at a speed of 95 mm/s. The recorded signals were later digitized with a 10-bit A-D converter and processed on a PDP 11/45 computer.

Total solar radiation was obtained from two identical pyranometers located a small distance away from the mast. Net radiation data were obtained from the CSIRO radiation measurements.

RESULTS AND DISCUSSION

Averages, taken every half hour (unfortunately, we did not have any control in the setting of this time), of mean velocity and temperature were recorded. From the mean velocity and temperature profiles (Figure 1) the gradient Richardson number was determined from the approximate relation

$$Ri(z) = [(g/\theta)(\partial\theta/\partial z)]/(\partial U/\partial z)^2$$

where θ is the potential temperature. Here, all the gradients were evaluated, at the geometric mean height, according to the equation

$$|\partial U/\partial z|_{z=(z_1z_2)^{1/2}} = \frac{U(z_2) - U(z_1)}{(z_1z_2)^{1/2} \ln (z_2/z_1)}$$

and a similar equation for $\partial\theta/\partial z$. The friction velocity U_*

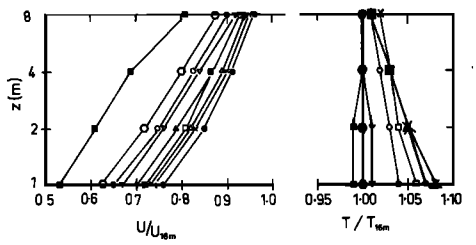

Fig. 1. Mean velocity and temperature profiles normalized by values at a height of 16 m. Symbols denote the following profiles: solid circles, 1400–1430 hours, U_{16m} = 6.6 m/s, T_{16m} = 20.98°C; crosses, 1400–1430 hours, U_{16m} = 6.91 m/s, T_{16m} = 21.27°C; open triangles, 1500–1530 hours, U_{16m} = 6.42 m/s, T_{16m} = 21.22°C; open squares, 1530–1600 hours, U_{16m} = 5.83 m/s, T_{16m} = 21.20°C; open circles, 1600–1630 hours, U_{16m} = 4.87 m/s, T_{16m} = 20.94°C; solid triangles, 1630–1700 hours, U_{16m} = 4.93 m/s, T_{16m} = 20.32°C; inverted open triangles, 1700–1730 hours, U_{16m} = 4.92 m/s, T_{16m} = 20.03°C; hexagons, 1730–1800 hours, U_{16m} = 4.35 m/s, T_{16m} = 19.84°C; solid squares, 1800–1830 hours, U_{16m} = 4.54 m/s, T_{16m} = 19.10°C.

(= $-\langle uw\rangle^{1/2}$, w being the vertical velocity fluctuation) and the friction temperature T_* (= $-\langle w\theta\rangle/U_*$) shown in Figure 2 were obtained from the relations

$$(\kappa z/U_*)(\partial U/\partial z) = \phi_m(z/L)$$

$$(\kappa Z/T_*)(\partial\theta/\partial z) = \phi_h(z/L)$$

where L is the Monin-Obukhov length. The Karman constant κ is here taken as 0.4, and the function ϕ_m and ϕ_h are approximated by [*Yaglom*, 1977]

$$\phi_m(z/L) = 1.14(1 - 13.1z/L)^{-1/4}$$

$$\phi_h(z/L) = 0.84(1 - 7.9z/L)^{-1/2}$$

for unstable conditions and by

$$\phi_m(z/L) = 1.14(1 + 4.1z/L)$$

$$\phi_h(z/L) = 1.14(0.74 + 4.1z/L)$$

for stable conditions ($0 < z/L < 1$). The stability parameter

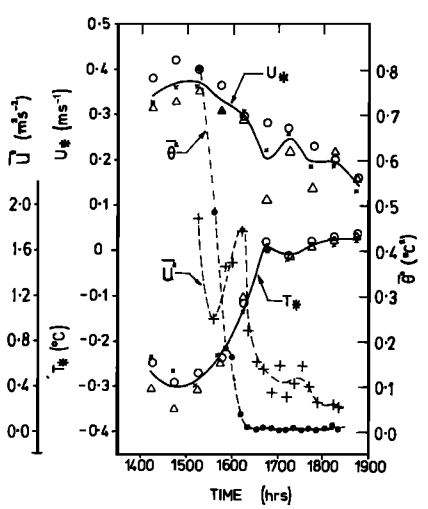

Fig. 2. Variation of U_* and T_* inferred from pairs of points on mean velocity and temperature profile. Geometric mean of pairs of points: open circles, 1.4 m; crosses, 2.8 m; open triangles, 5.6 m. Solid curves refer to averaged values. (The variation of $\langle u^2\rangle$ and $\langle\theta^2\rangle$ at a height of 4 m: pluses, $\langle u^2\rangle$; solid circles, $\langle\theta^2\rangle$. Average values in the figure are denoted by angle brackets in the text.)

z/L (shown in Figure 3 for z = 4 m) was obtained from the relation $z/L = (\phi_m^2/\phi_h)\,Ri$.

Strictly speaking, the above relations are not likely to be valid immediately following a step change in the surface heat flux, since they have been derived for near-equilibrium conditions. Diffusion of $\langle\theta^2\rangle$ within the internal thermal layer is likely to be a significant part of the $\langle\theta^2\rangle$ budget [e.g., *Townsend*, 1976, equation 8.3.4] and may lead to an inequality between production and dissipation terms. The propagation velocity of this layer can be written [e.g., *Antonia et al.*, 1977] as

$$d\delta_T/dt = a_{1\theta}U_*$$

where $a_{1\theta} = \langle w\theta\rangle/\langle\theta^2\rangle^{1/2}\langle -uw\rangle^{1/2} = T_*/\langle\theta^2\rangle^{1/2}$ is approximately 0.5 for conditons ($z/L \simeq -0.3$) prevailing before the change. For $U_* \simeq 0.3$ m/s, $d\delta_T/dt \simeq 0.15$ m/s, which is a relatively rapid propagation rate of the edge of the internal layer.

For the present temporal variation of the incoming solar radiation Q_w (Figure 3*b*) we can follow *Wyngaard*'s [1973] example by considering whether the surface layer turbulence follows a continuum of equilibrium states in response to changes in stability brought about by the change in Q_w. A characteristic time τ_{Q_w} for solar radiation is

$$\tau_{Q_w} = |Q_w/(\partial Q_w/\partial t)|$$

For the distribution (Figure 3*b*) of Q_w during the eclipse, τ_{Q_w} is about 2 hours at 1600 hours. (Note that for the distribution of Q_w on a normal day, τ_{Q_w} is significantly larger, being about 4 hours at 1600 hours.) A characteristic response time for the turbulence may be written, in the case of $\langle\theta^2\rangle$, as

$$\tau_{\langle\theta^2\rangle} = -\langle\theta^2\rangle/\langle w\theta\rangle(\partial T/\partial z) \qquad (1)$$

In the case of $\langle q^2\rangle$ (the turbulent kinetic energy),

$$\tau_{\langle q^2\rangle} = \langle q^2\rangle/\langle -uw\rangle(\partial U/\partial z)(1 - R_f) \qquad (2)$$

where R_f is the flux Richardson number:

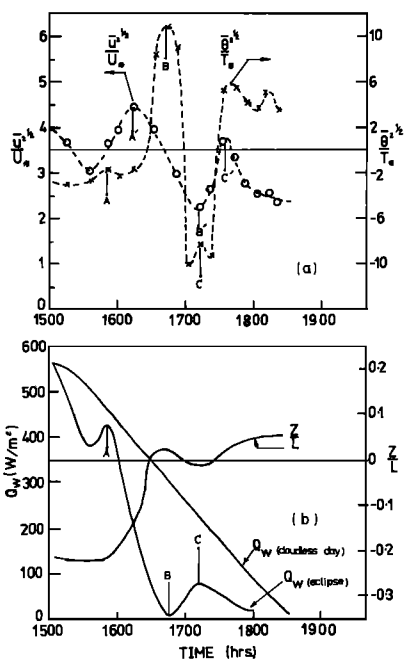

Fig. 3. Variation of total radiation, rms velocity, and rms temperature at a height of 4 m. (The variation of z/L shown refers to z = 4 m and a value of L taken as the average of values at 1.4 m, 2.8 m, and 5.6 m. Average values in the figure are denoted by angle brackets in the text.)

$$R_f = -\frac{g}{T}\frac{\langle w\theta\rangle}{\langle -uw\rangle(\partial U/\partial z)}$$

(1) and (2) may be rewritten as

$$\tau_{\langle\theta^2\rangle} = (\beta\kappa_\theta z)/(U_*\phi_h)$$

and

$$\tau_{\langle q^2\rangle} = \frac{(\alpha\kappa z)}{U_*[\phi_m - (z/L)]}$$

where it is assumed that $\langle q^2\rangle = \alpha U_*^2$ and $\langle\theta^2\rangle = \beta T_*^2$. At $z = 4$ m($z/L \simeq -0.3$), $\tau_{\langle\theta^2\rangle}$ and $\tau_{\langle q^2\rangle}$ are equal to 50 s and 60 s, respectively, when $\alpha \simeq 7.5$ and $\beta \simeq 4$. These times are significantly smaller than the previously mentioned value of τ_{Q_w} at 1600 hours. An averaging time of 10 min was used to determine $\langle u^2\rangle$ and $\langle\theta^2\rangle$ in Figure 3*a*. This time is large enough in relation to $\tau_{\langle\theta^2\rangle}$ or $\tau_{\langle q^2\rangle}$ but is relatively small in comparison to most values of τ_{Q_w}. Running mean values of u^2 and θ^2 suggest that there is satisfactory convergence for most records to a final value within the 10-min period. At 1658 hours, where the gradient $\partial Q_w/\partial t$ is largest, $\tau_{Q_w} \simeq 15$ min, and the accuracy of the averages near this time is likely to be poor.

The almost immediate response of the temperature field to the change in ground heat flux is clearly evident in the results of Figures 1–3. Figure 1 shows a noticeable decrease in the temperature near the surface during the early (1600–1630 hours) part of the eclipse. During the period in which the incoming radiation is essentially zero, the temperature is constant. The subsequent increase (1700–1730 hours) in solar radiation is reflected by the increase in T close to the surface. At later times the temperature profile becomes stable. The variation of $\langle\theta^2\rangle^{1/2}$ follows that of Q_w quite closely, and the positions of the extrema in $\langle\theta^2\rangle^{1/2}/T_*$ (marked A, B, and C in Figure 3*a*) are essentially identical with the corresponding positions of Q_w in Figure 3*b*. The maximum value of $\langle\theta^2\rangle^{1/2}/T_*$ at B (Figure 3*a*) is of course due to the very small (positive) value of T_* at that position (see Figure 2). The decrease in $\langle u^2\rangle^{1/2}$ over the early part of the eclipse is significantly slower than that of $\langle\theta^2\rangle^{1/2}$. To within the scatter in the data the positions of extrema (denoted by A', B', and C' in Figure 3*a*) of $\langle u^2\rangle^{1/2}/U_*$ lag behind the corresponding extrema positions of $\langle\theta^2\rangle^{1/2}/T_*$ by almost 20 min. The behavior of the variation of $\langle u^2\rangle^{1/2}/U_*$ and $\langle\theta^2\rangle^{1/2}/|T_*|$ with respect to z/L is not significantly different from that measured during normal days. This suggests that the concept of Monin-Obukhov similarity, to the extent that it can be trusted, provides a reasonable description of the behavior of turbulence properties during the eclipse. This latter observation provides further justification for the suggestion that the response of surface layer turbulence to the eclipse proceeds via a series of equilibrium steps. It must also be mentioned that variations in $\langle u^2\rangle^{1/2}$ and $\langle\theta^2\rangle^{1/2}$ at 2 m (not shown here) are essentially identical with those at 4 m, which are consistent with the previously indicated large speed of propagation of the internal layer.

It may be of interest to verify the existence of an inertial subrange for one-dimensional velocity and temperature spectra, especially if such information were to be used for the determination of U_* and T_*, by way, for example, of the inertial dissipation technique [e.g., *Champagne et al.*, 1977]. The one-dimensional velocity spectrum $\phi_u(k_1)$, defined such that $\int_0^\infty \phi_u(k_1)dk_1 = \langle u^2\rangle$ (k_1 is the wave number $2\pi n/U$), exhibits a well-defined inertial subrange (Figure 4*a*) for the entire period for which measurements were taken. The values of U_* inferred from the inertial dissipation technique are in reasonable agreement with those given in Figure 2. In the case of $\phi_\theta(k_1)$ the inertial subrange (Figure 4*b*) is reasonably well established for the period (1610–1620 hours) near the start of the eclipse, even though $\langle\theta^2\rangle$ has started to decrease appreciably in response to the decrease in Q_w (Figure 2). At later times the inertial subrange is first confined only to the range $6 < k_1z < 20$ and disappears at 1800 hours. We do not have an explanation for the increase in the function $\phi_\theta(k_1z)^{5/3}$ over wave numbers greater than those for which an inertial subrange still exists. It should be pointed out, however, that such an increase, prior to the expected decrease as the Kolmogorov wave number is approached, has been observed, under normal conditions, by *Champagne et al.* [1977] and *Williams and Paulson* [1977]. This increase was not evident in temperature spectra taken prior to the eclipse.

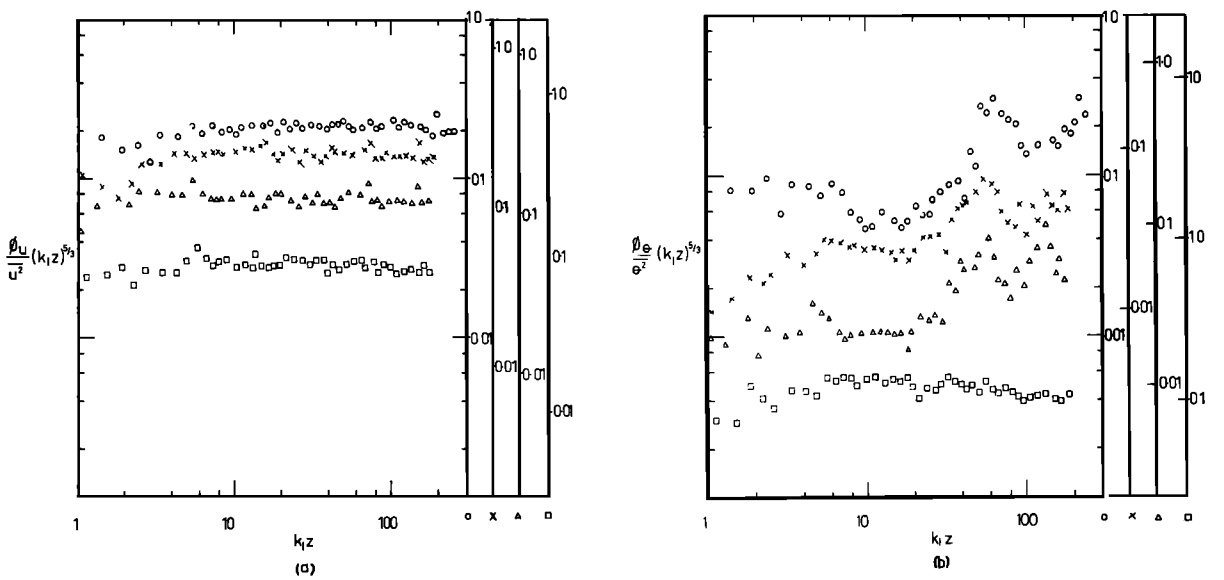

Fig. 4. Power spectral densities of velocity and temperature weighted by $(k_1z)^{5/3}$ at a height of 4 m. Figure 4*a* refers to u, and Figure 4*b* refers to θ. Circles indicate, 1757–1807 hours; crosses, 1707–1717 hours; triangles, 1637–1647 hours; and squares, 1607–1617 hours. (Average values in the figure are denoted by angle brackets in the text.)

Acknowledgments. The authors are grateful to A. Dyer of the CSIRO Department of Atmospheric Physics (Aspendale) for the invitation to participate in the 1976 International Turbulence Comparison Experiment and for the mean velocity and temperature data. The authors are also grateful to the Newcastle Broadcasting and Television Corporation Ltd., for the use of the environmental measurement unit during the period of the experiment. The support of the Australian Research Grants Committee is gratefully acknowledged.

REFERENCES

Antonia, R. A., H. Q. Danh, and A. Prabhu, Response of a turbulent boundary layer to a step change in surface heat flux, *J. Fluid Mech., 80,* 153–177, 1977.

Champagne, F. H., C. A. Friehe, and J. C. La Rue, Flux measurements, flux estimation techniques, and fine-scale turbulence measurements in the unstable surface layer over land, *J. Atmos. Sci., 34,* 515–530, 1977.

Nicholl, C. I. H., Some dynamical effects of heat on a turbulent boundary layer, *J. Fluid Mech., 40,* 361–384, 1970.

Townsend, A. A., Turbulent flow in a stably stratified atmosphere, *J. Fluid Mech., 3,* 361–372, 1957.

Townsend, A. A., *The Structure of Turbulent Shear Flow,* 2nd ed., Cambridge University Press, New York, 1976.

Trainor, J. B., October's total solar eclipse in Australia, *Sky Telescope, 51,* 300–306, 1976.

Williams, R. M., and C. A. Paulson, Microscale temperature and velocity spectra in the atmospheric boundary layer, *J. Fluid Mech., 83,* 547–567, 1977.

Wyngaard, J. C., On surface-layer turbulence, in *Workshop on Micrometeorology,* edited by D. A. Haugen, pp. 101–176, American Meteorological Society, Boston, Mass., 1973.

Yaglom, A. M., Comments on wind and temperature flux-profile relationships, *Boundary Layer Meteorol., 11,* 85–102, 1977.

(Received January 30, 1978;
revised October 5, 1978;
accepted October 16, 1978.)